Application of a Hybrid FEM/MOM Method to a Canonical PCB Problem

Y. Ji, J. Chen, T. H. Hubing, J. L. Drewniak
Electromagnetic Compatibility Laboratory
Department of Electrical & Computer Engineering
University of Missouri-Rolla
Rolla, MO 65401

Abstract: In this paper a hybrid FEM/MOM method was used to solve a canonical printed circuit board (PCB) problem. The PCB is populated with three traces. One is a signal line and the other two are I/O lines that extend beyond the boundary of the board. The Finite Element Method (FEM) was used to model the fields in the volume around the on-board trace. The Method of Moments (MOM) was employed to model the equivalent surface currents on the board and the current on the off-board traces. The FEM and MOM equations were coupled by forcing the continuity of tangential fields on the dielectric boundary. An efficient meshing strategy was employed to reduce the memory requirements. Major contributors to far fields in different frequency bands and for different polarizations are discussed.

PROBLEM DESCRIPTION

The problem investigated in this article was proposed at the 1998 IEEE International Symposium on Electromagnetic Compatibility. Solutions using the Finite-Difference Time-Domain (FDTD) method [1], the Partial Element Equivalent Circuit (PEEC) method [2], and the Transmission-Line (TLM) method [3] were presented by researchers. However, no consensus had been reached on the solutions. The problem configuration is shown in Figures 1 and 2. Figure 1 provides a three-dimensional view of the PCB. Figure 2 shows the top view. The PCB is 25 cm long, 25 cm wide and 0.8 mm thick. The board is covered by dielectric with a relative permittivity of 4.5. The bottom side of the board is a metal plane with a gap 12cm long and 1.0 cm wide. On the top side of the board there are three printed traces. One is a signal line. The other two are I/O traces that extend beyond the boundary of the board. The signal trace is fed at Point 1 by a periodic trapezoidal 10-Ω voltage source, with the waveform shown in Figure 3. It is terminated by a 55-Ω resistor at Point 4 to the metal plate. The two I/O traces are terminated at Points 2 and 3 by two 55-Ω resistors.

The primary challenge of this problem is the mixed physical scales. The width of the traces is 0.2 mm and they are spaced by 0.2 mm. The board thickness is 0.8 mm. On the other hand, the board size is 25×25 cm^2 and the total length of the I/O traces is more than 100 cm.

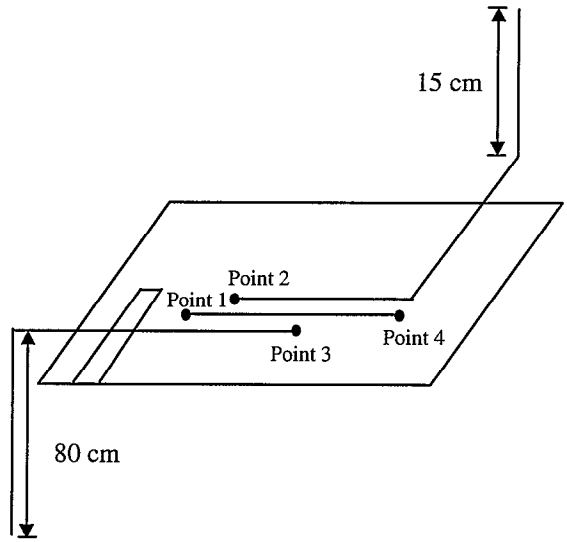

Figure 1. A printed circuit board with three traces.

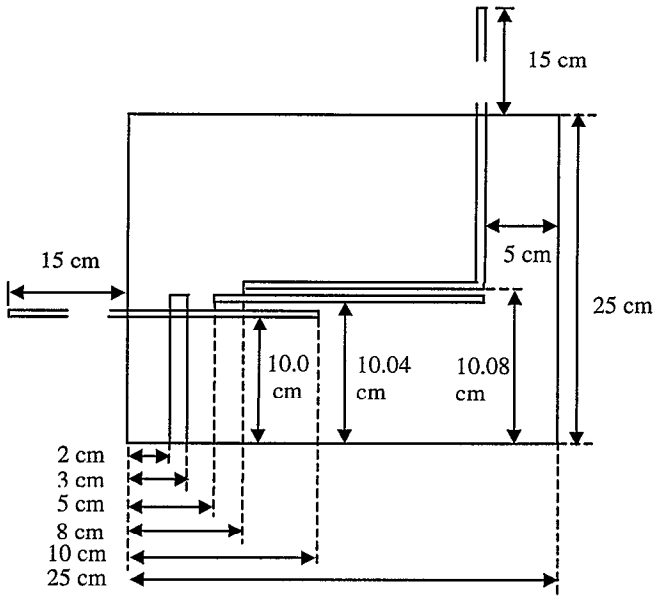

Figure 2. Top view of the board.

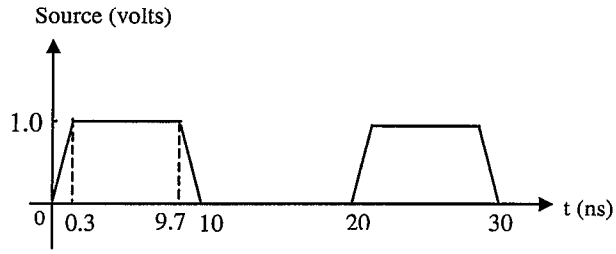

Figure 3. The input waveform at Point 1.

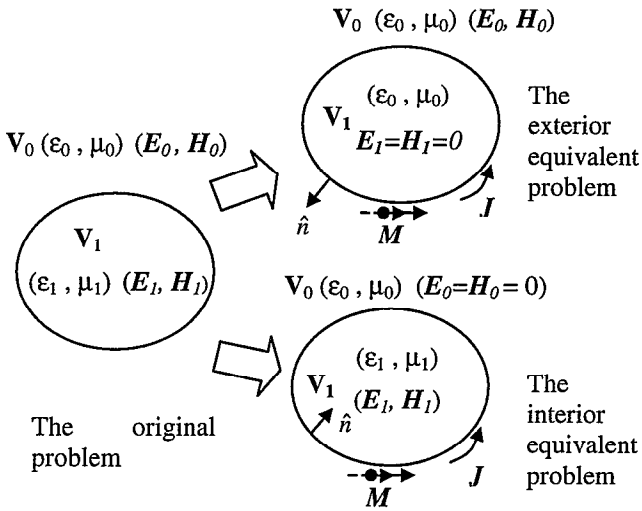

Figure 4. The original problem can be decomposed into the exterior equivalent and the interior equivalent problems.

FEM/MOM FORMULATION

Full-wave hybrid FEM/MOM methods are well suited for solving problems that combine inhomogeneous regions with small structures and larger radiating conductors. They have been successfully used to solve scattering problems in the antenna community [4][5] and have also been applied to the analysis of radiation from printed circuit board geometries [6][7][8][9].

The problem of interest is shown in Figure 4. The problem consists of two volumes, V_0 and V_1, which have different constitution parameters (ε_0 , μ_0) and (ε_1 , μ_1), respectively. (ε_0 , μ_0) are constants, while (ε_1 , μ_1) can be a function of position. According to the equivalence principle [10][11], the problem in Figure 4 can be decomposed into two problems: the exterior equivalent problem and the interior equivalent problem. To solve for the fields (E_0, H_0) in V_0, equivalent electric currents J and equivalent magnetic currents M are introduced to positions just above the fictitious boundary between V_0 and V_1. All fields in V_1 are set to zero. Because the new problem gives the same fields (E_0, H_0) in volume V_0 as the original problem does, it is called the exterior equivalent problem of the original one. Since the fields in V_1 are zero, the fields in V_0 are not affected no matter what kind of materials are in V_1. Thus, V_1 can be filled with the materials with (ε_0 , μ_0) [11]. Now, the exterior equivalent problem is a homogeneous problem. The homogenous Green's function can be used as the kernel to formulate an integral equation and the Method of Moments (MOM) can be used to solve it. Similarly, for the interior equivalent problem, the fields in V_0 are set to zero while surface currents J and M are introduced on the boundary to solve the field (E_1, H_1) in V_1. The finite element method (FEM) is employed to analyze the interior equivalent problem. The two equivalent problems are related by forcing the continuity of tangential fields.

The integral equation describing the exterior equivalent problem is given by [10],

$$\mathbf{E}(\mathbf{r}) = \mathbf{E}^{inc} + \int_S \{ \mathbf{M}(\mathbf{r}') \times \nabla' G_0(\mathbf{r},\mathbf{r}') + j k_0 \eta_0 \mathbf{J}(\mathbf{r}') G_0(\mathbf{r},\mathbf{r}') + j \frac{\eta_0}{k_0} \nabla' \bullet \mathbf{J}(\mathbf{r}') \nabla G_0(\mathbf{r},\mathbf{r}') \} dS' \quad (1)$$

where k_0 and η_0 are the wavenumber and the wave impedance in the volume V_0. The three-dimensional homogeneous Green's function is given by,

$$G_0(\mathbf{r},\mathbf{r}') = \frac{e^{-j k_0 |\mathbf{r}-\mathbf{r}'|}}{4\pi |\mathbf{r}-\mathbf{r}'|} .$$

Triangular basis functions are employed to approximate surface fields. A Galerkin's procedure is used to test the integral equation, which implies that weighting functions are chosen from the same set of basis functions.

The weak form used to describe the interior equivalent problem is given by [7],

$$\int_{V_1} \left[\left(\frac{\nabla \times \mathbf{E}(\mathbf{r})}{j\omega\mu_0\mu_r} \right) \bullet (\nabla \times \mathbf{w}(\mathbf{r})) + j\omega\epsilon_0\epsilon_r \mathbf{E}(\mathbf{r}) \bullet \mathbf{w}(\mathbf{r}) \right] dV = \int_{S_1} (\hat{\mathbf{n}} \times \mathbf{H}(\mathbf{r})) \bullet \mathbf{w}(\mathbf{r}) \, dS - \int_{V_1} \mathbf{J}^{int}(\mathbf{r}) \bullet \mathbf{w}(\mathbf{r}) \, dV \quad (2)$$

where S_1 is the surface enclosing volume V_1, $\mathbf{w}(\mathbf{r})$ is the weighting function, and $\mathbf{J}^{int}$ is the impress source.

For this problem, the boundary chosen to apply the integral equation is shown in Figure 5. The boundary coincides with the physical boundary of the board. The boundary also includes the off-board traces. One advantage of this formulation is that the off-board traces are treated in the exterior equivalent problem without introducing white-space.

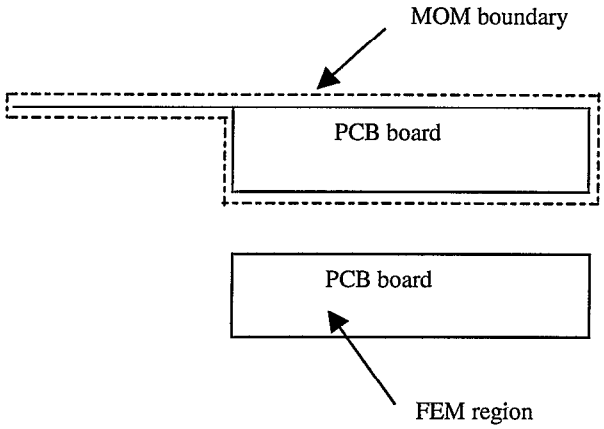

Figure 5. The MOM and FEM regions.

Only the electric currents along the off-board traces are unknowns. Because the traces are very thin, they are treated as Perfect Electric Conductors (PEC) with infinitesimal thickness.

MESHING STRATEGY

The primary challenge of this problem is its wide range of physical scales. Triangular and tetrahedral elements have advantages of approximating arbitrary geometries effectively and efficiently. But the MOM puts a constraint on the total number of triangular elements. MOM requires $O(N^2)$ memory and $O(N^3)$ computation time. Double precision data types are used to store the MOM matrix coefficients. Each entry of the matrices is a complex number, thus requiring 16 bytes of computer memory. Therefore, 3,000 unknowns on the MOM boundary require more than 140M bytes of computer memory. The computation time for one frequency with 3,000 unknowns takes about 10 hours on a Pentium 450 MHz personal computer. Thus, practically, the number of unknowns (edges) on the MOM boundary cannot exceed 3,000. On the other hand, the finite element method requires O(N) memory and relatively little computation time per unknown since it generates highly sparse matrices. Therefore, a key to this problem is to reduce the unknowns on the MOM boundary.

The main factor determining the meshing quality is the aspect ratio of the triangular and tetrahedral elements. To maintain the quality of tetrahedral elements, small triangular elements must be used to discretize the boundary, which in consequence leads to a large number of boundary edges. The MOM equation, Eq. (1), and the FEM equation, Eq. (2), are coupled by forcing tangential field continuity on the dielectric surface. As illustrated in Figure 6, S^+ denotes the dashed circle, which is the MOM boundary; S^- denotes the solid circle, which is the FEM boundary. With the presence of a PEC surface, which is denoted as S_c^+ on the MOM boundary and S_c^- on the FEM boundary, the MOM equation in Eq. (1) models the current on S_c^+ but not the current on S_c^-. The triangular elements on S_c^+ do not need to match the tetrahedral elements meshed along S_c^-. Therefore, it is possible to use different mesh sizes on S_c^+ and S_c^-. The edges on S_c^- are not unknowns in FEM equation because the E fields along those edges are forced to be zero. Using small mesh elements on S_c^- produces a tetrahedral mesh of good quality but does not increase the number of boundary elements in the MOM equation.

The problem can also be truncated to reduce boundary edges. As shown in Figure 7, the ratio of the trace width to the size of the ground plane is 1/1250 but the three traces are closely spaced. Fields change rapidly around the traces, but they are small and vary smoothly in other places. For this reason, only the dielectric around the traces is modeled to reduce unknowns on the MOM boundary. Figure 8 shows the cross-sectional view of the truncated problem for the region where signal on the active trace is coupled to I/O lines. Rather than modeling the whole dielectric slab, the width of the dielectric slab was changed to 15 W. The ground plane was kept intact since it may have a significant effect on the radiation resistance of the long off-board traces.

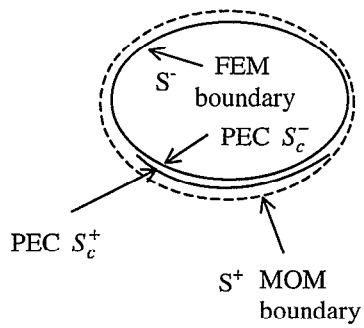

Figure 6. FEM boundary and MOM boundary near a PEC.

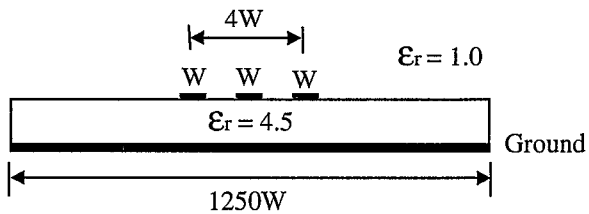

Figure 7. Cross-sectional view of the three coupled traces.

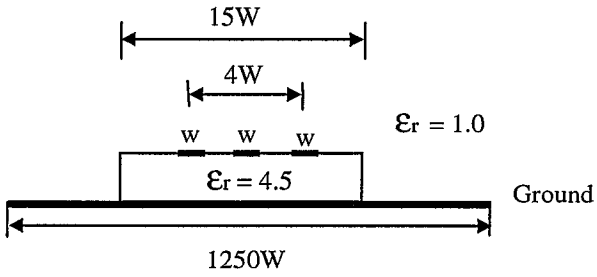

Figure 8. Cross-sectional view of the truncated problem.

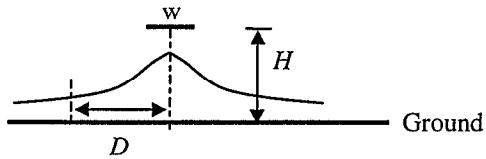

Figure 9. High-frequency current distribution under a trace.

The high-frequency current distribution underneath a trace is shown in Figure 9. The current density peaks directly under the trace, then falls off sharply to each side. The current density at a point D meters away from the center of the trace is given by,

$$J(D)=\frac{I_0}{\pi H}\bullet\frac{1}{1+(\frac{D}{H})^2}$$

where I_0 is the current on the trace, H is the height of trace above the ground plane and D is the distance from the trace. Because the majority of the current flows underneath the trace, the element size on the ground plane is linearly biased from a fine mesh underneath the trace to a large coarse mesh far away from the trace.

NUMERICAL RESULTS

A commercial mesh generator was used to generate the mesh for this problem. Table I summarizes the tetrahedral elements used to discretize the FEM volume. The inner edges are defined as edges located inside the FEM volume. Those edges are modeled by the FEM equation and only require a small amount of computer memory. The boundary edges are included in both the FEM and MOM equations. The aspect ratio of the tetrahedral elements is crucial to the accuracy of the results, so the mesh generator was instructed to maintain an aspect ratio less than 6 for all tetrahedra. Table II summarizes the triangular mesh on the MOM surface. The triangular elements on the on-board traces are critical, so a fine mesh is employed. Larger triangles are used to mesh the off-board traces. Currents on the trace change rapidly near the edge of the ground plane and near the gap region, so fine elements are employed in those places.

The periodic excitation at Point 1 was transformed to the frequency domain using an FFT. The duration of the signal is 20 ns, therefore the fundamental frequency is 50 MHz. In this paper, the solution was obtained at each of the first 20 harmonics. The hybrid FEM/MOM code required 115 minutes to iterate one frequency on a Pentium 450 personal computer. The total memory required was 101 Mbytes and the total computation time for all frequencies was 40 hours.

Table 1. Summary of tetrahedral mesh in the FEM volume.

Number of tetrahedrons	Number of inner edges	Number of boundary edges	Total number of unknown edges	Aspect ratio of tetrahedra (maximum)	Tetra collapse (maximum)
1238	664	1003	1667	5.55	0.22

Table 2. Summary of triangular mesh on the MOM boundary.

	Number of triangles used	Number of edges	Aspect ratio of triangles(maximum)	Skew angle (maximum degree)
Dielectric surface	1003	833	5.10	77
On-board traces	327	331	10.05	78
Off-board traces	292	294	66.7	90
Ground plane	235	165	2.75	60

Figure 10 illustrates the maximum electric field computed 10 meters from the board when the input signal shown in Figure 3 is applied at Point 1. This board fails to meet the FCC Class A limit. It exceeds the limit in the 500-700 MHz frequency range. Figures 11 and 12 show the computed maximum horizontal and vertical electric fields 10 meters from the board when the amplitude of each source harmonic is normalized to 1 volt. The hybrid code allows the user to calculate how much of the total field emanates from individual portions of the geometry. Far fields generated by different portions of the structure are compared in these two figures. The lines referred to in Figures 11 and 12 are defined as follows,

Line 1: the 80cm long vertical off-board trace.

Line 2: the 15cm long horizontal off-board trace at the left side in Figure 2.

Line 3: the 15cm long horizontal off-board trace at the top-right corner in Figure 2.

Line 4: the 15cm long vertical off-board trace.

Figure 11 shows that the board itself is the major contributor to the horizontally polarized radiation. Figure 12 illustrates the different contributions to the vertical electric fields. It indicates that below 500 MHz, Line 1 is the dominating contributor. At frequencies above 500 MHz, Line 2 is the dominant contributor. The radiated field peaks at 550 MHz. This corresponds to the half-wavelength resonance of the active trace.

Figure 13 demonstrates the effect that the gap in the ground plane has on the calculated field. With the gap removed, radiation below 500 MHz is increased slightly. Above 500 MHz however, the gap appears to increase the radiated field levels.

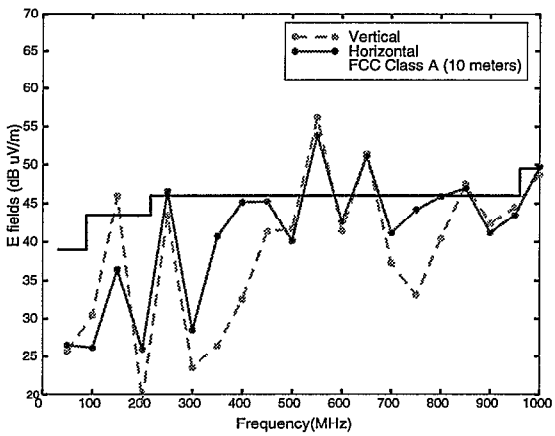

Figure 10. The maximum 10-meter electric field.

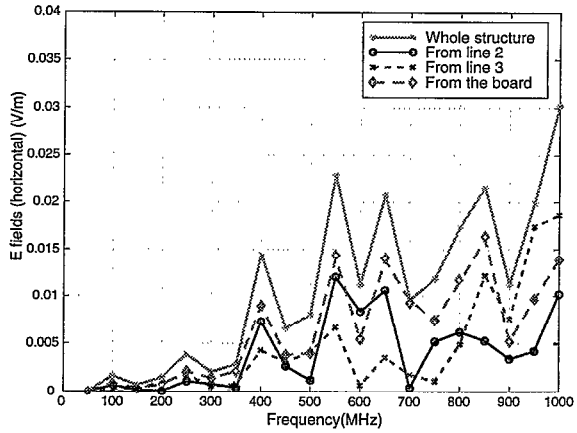

Figure 11. The maximum horizontal electric field 10 meters from the board with a normalized source.

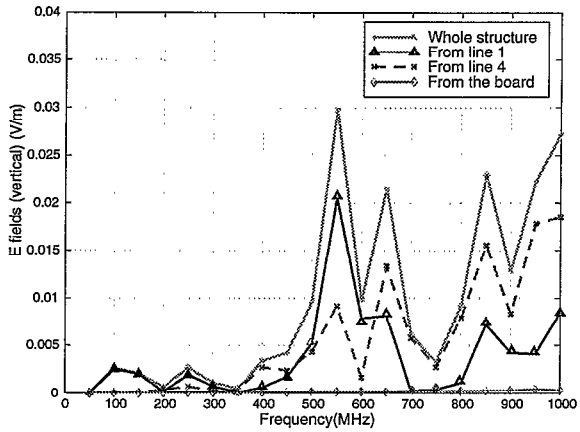

Figure 12. The maximum vertical electric field 10 meters from the board with a normalized source.

CONCLUSION

In this paper, a hybrid FEM/MOM method was employed to analyze a canonical printed circuit problem. The MOM can model the off-board traces without introducing any white-space. The FEM can model the fields around the traces without excessive memory requirements. For the analysis presented here, a commercial mesh generator was used to discretize the surface and volume efficiently. To conserve memory, the dielectric was modeled only in the region 15 trace widths around the signal and I/O traces. Numerical results in the frequency domain are presented.

Although this paper presents a calculated electric field value relative to the FCC emission limit, numerical modeling codes are not particularly useful for this purpose. Small changes in a particular geometry can have a dramatic effect on the calculated field at any given

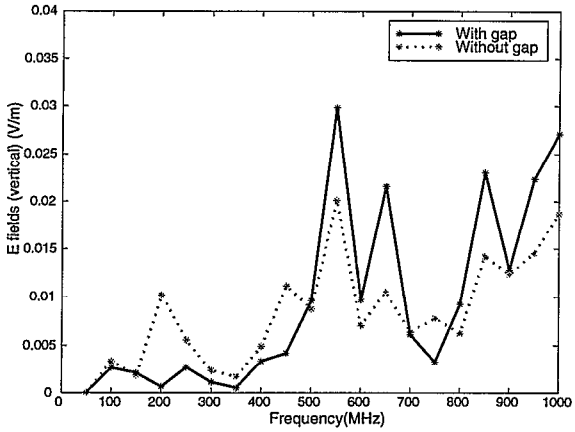

Figure 13. The maximum vertical electric field 10 meters from the board with and without the gap.

frequency. For example, a slight change in the way a cable is modeled could mean the difference between being resonant at a source harmonic or a few MHz off a source harmonic. The calculated field strength could easily vary by 20 dB or more due to this slight change.

The main advantage of numerical models is that they can tell us things about the way a given configuration radiates that we could never learn from measurements. In the example presented here, the parts of the structure that contributed most significantly to the radiated field at different frequencies were identified. Also the effect of the gap in the ground plane was explored.

The hybrid MOM/FEM approach was well suited to this problem. The region around the signal and I/O traces was meshed with many small FEM elements and the cables and other areas of the board were meshed with relatively large MOM elements. As a result, this complex problem was able to be modeled efficiently on a modestly equipped personal computer.

REFERENCES

[1] Jason Mix, Gary Haussmann, Melinda Piket-May and Kevin Thomas, "EMC/EMI Design and Analysis Using FDTD", *Proceedings of the 1998 IEEE International Symposium on Electromagnetic Compatibility*, vol. 1, pp. 177-181, Denver, CO, August 1998.

[2] Albert E. Ruehli and Andreas C. Cangellaris, "Application of the partial Element Equivalent Circuit (PEEC) method to realistic printed circuit board problem", *Proceedings of the 1998 IEEE International Symposium on Electromagnetic Compatibility*, vol. 1, pp. 182-187, Denver, CO, August 1998.

[3] C. Christopoulos, "Application of the TLM Method to Equipment Shielding Problems", *Proceedings of the 1998 IEEE International Symposium on Electromagnetic Compatibility*, vol. 1, pp. 182-187, Denver, CO, August 1998.

[4] X. C. Yuan, D. R. Lynch, and J. W. Strohbehn, "Three-dimensional Finite, Boundary, and Hybrid Element Solutions of the Maxwell's Equations for Lossy Dielectric Media," *IEEE Trans. on Microwave Theory and Tech.*, vol. 36, pp. 682-693, April 1988.

[5] Jian-Ming Jin and John L. Volakis, "Electromagnetic Scattering by and Transmission Through a Three-dimensional Slot in a Thick Conducting Plane," *IEEE Trans. on Antennas and Propagat.*, vol. 39, pp. 543-550, April 1991.

[6] Mohammad W. Ali, "Development of A Hybrid 3D Numerical Modeling Technique for Analyzing Printed Circuit Models with Attached Wires," Ph.D. dissertation, University of Missouri-Rolla, December 1996.

[7] M. W. Ali, T. H. Hubing and J. L. Drewniak, "A Hybrid FEM/MOM Technique for Electromagnetic Scattering and Radiation from Dielectric Objects with Attached Wires," *IEEE Trans. on Electromagnetic Compatibility*, vol. 39, pp. 304-314, November 1997.

[8] Y. Ji, M. Ali, T. H. Hubing, "EMAP5: A 3D Hybrid FEM/MOM Code", *Proceedings of the 14th Annual Review of Progress in Applied Computational Electromagnetics*, pp. 928-935,Monterey, CA, March 1998.

[9] Y. Ji, M. Ali and T. H. Hubing, "EMC Applications of the EMAP5 Hybrid FEM/MOM Code", *Proceedings of the 1998 IEEE International Symposium on Electromagnetic Compatibility*, vol. 1, pp. 177-181, Denver, CO, August 1998.

[10] Johnson J. H. Wang, *Generalized Moment of Methods in Electromagnetics*, New York: John Wiley & Sons, 1990.

[11] Andrew F. Peterson, Scott L. Ray and Raj Mittra, Computational Methods for Electromagnetics, Oxford University Press and IEEE Press, 1998.